JOURNAL OF VIROLOGY, Oct. 1977, p. 326-342

Vol. 24, No. 1
Printed in U.S.A.

Macromolecular Synthesis in Cells Infected by Frog Virus 3

VII. Transcriptional and Post-Transcriptional Regulation of Virus Gene Expression

D. B. WILLIS,* R. GOORHA, M. MILES, AND A. GRANOFF

Division of Virology, St. Jude Children's Research Hospital, Memphis, Tennessee 38101

Received for publication 28 April 1977

We have used improved techniques for separating individual species of RNA and protein to study the mechanisms that control gene expression by frog virus 3, a eucaryotic DNA virus. Forty-seven species of viral RNA and 35 viral polypeptide species were resolved by polyacrylamide gel electrophoresis. The relative molar ratios of virus-specific polypeptides synthesized at various times after infection were determined by computer planimetry and were compared with the molar ratios of appropriate-sized viral RNAs to code for each polypeptide. Viral polypeptides were classified according to the time during the growth cycle at which their maximal rate of synthesis occurred—early, 2 to 2.5 h; intermediate, 4 to 4.5 h; and late, 6 to 6.5 h. The viral RNAs, which were assumed to be mRNA's, could not be classified according to time of maximum synthesis; once their synthesis had begun, most of the RNAs continued to be synthesized at the same or higher rates. However, only 10 of the 47 viral RNA bands were plainly visible after electrophoresis of extracts from cells labeled from 1 to 1.5 h after infection; these 10 RNAs were designated "early" RNA. The early pattern of both RNA and polypeptide synthesis was maintained for at least 6 h in the presence of the amino acid analog fluorophenylalanine, which indicates that a functional viral polypeptide was required for "late" transcription and translation. The presumptive mRNA's for late polypeptides did not appear until 2 h after infection, but two of these "late" RNAs became the major products of transcription by 4 h into the infectious cycle. In contrast to the declining rate of synthesis of the early proteins, corresponding early RNA species continued to be synthesized at the same or higher rates throughout the replicative cycle. Although the synthesis of late virus-specific proteins appeared to be regulated at the level of transcription, our results suggest that the synthesis of both early and intermediate proteins was regulated at the post-transcriptional level.

With a requirement for a nuclear function (11) but with maturation in the cytoplasm (12), frog virus 3 (FV 3) differs in mode of replication from all other known DNA viruses. This virus has several unusual features that assist in analysis of virus-directed macromolecular syntheses. Treatment of host cells with heat-inactivated FV 3 (ΔFV 3) suppresses host RNA, DNA, and protein synthesis without affecting the subsequent replication of active virus (8, 33). Therefore, very early viral events are unmasked in the absence of host cell macromolecular synthesis.

Virus-specific polypeptide synthesis proceeds in a sequentially controlled fashion during the growth cycle of wild-type FV 3 (8). Goorha and Granoff (8) demonstrated that one class of FV 3-specific proteins was synthesized at maximal rates at the beginning of infection (1 to 2 h), whereas other proteins attained their highest rates of synthesis toward the end of the growth cycle (6 to 8 h). The decrease in the rate of synthesis of at least one early protein appeared to be controlled at the post-transcriptional level. The increase in late protein synthesis was not dependent on viral DNA replication (8); therefore, we use the terms "early" (<2 h) and "late" (>6 h) in relation to time after infection rather than onset of DNA replication. In contrast to the orderly replication of wild-type virus, certain temperature-sensitive mutants of FV 3 exhibit deranged patterns of protein synthesis (10), providing evidence for the role of virus-specific regulatory factors in protein synthesis.

To define the role of transcriptional control in the regulation of FV 3 protein synthesis, Willis and Granoff (33) analyzed viral RNA on sucrose density gradients and by hybridization inhibition. The results suggested that the synthesis of

viral messages varied both qualitatively and quantitatively with time. However, because of the poor resolution of RNA obtainable on sucrose gradients, they could not determine the role of transcription in the regulation of any individual polypeptides. We have recently achieved sharp resolution of both polypeptides and RNAs with polyacrylamide gels, and we have used these techniques to compare directly the rates of synthesis of individual species of virus-specific RNA and the polypeptides for which each may code. Most of the FV 3 RNAs lack segments of polyadenylic acid [poly(A)] at their 3'-termini (34), and, as we will demonstrate, the absence of variable-length tracts of poly(A) permits superior resolution of viral RNA on formamide-polyacrylamide gels.

Our results clearly demonstrate that: (i) FV 3 RNA synthesis is controlled quantitatively—not all RNA species were synthesized in the same molar ratios; (ii) FV 3 RNA synthesis is controlled qualitatively—a virus-induced protein was required to turn on synthesis of late RNA; and (iii) post-transcriptional regulation is a major strategy for control of protein synthesis in the FV 3-infected cell—transcription of early RNA species continued unabated throughout infection.

MATERIALS AND METHODS

Cells and virus. Fathead minnow (FHM) cells were grown as monolayers at 33°C in Eagle minimum essential medium containing 10% fetal calf serum (MEM-10). A clonal isolate of FV 3 was grown and titrated in FHM cells at 25°C; concentrated virus stocks were prepared as described previously (22).

Reagents. [^{35}S]methionine (specific activity, 600 Ci/mmol) was produced by New England Nuclear Corp.; [^{3}H]uridine (specific activity, 20 Ci/mmol) was purchased from Schwarz/Mann. Formamide, obtained from BDH Laboratories, was deionized with 5% Amberlite MB-1 until the conductivity measured less than 3 mmho. All formamide solutions were stored at −20°C.

Isotopic labeling of virus-specific RNA and polypeptides in infected cells. To inhibit host RNA (33) and protein syntheses (8), we exposed cells to ΔFV 3 (56°C, 15 min) in amounts equivalent to 20 PFU/cell for 60 min at room temperature (23°C). The cells were then washed, overlaid with MEM-10, and incubated at 30°C for 2 h. The medium was removed, and active virus was adsorbed at 50 PFU/cell (23°C, 60 min). The cells were washed, overlaid with MEM without serum, and incubated at 30°C. This time was taken as 0 h for the infectious cycle. It was not necessary to use ΔFV 3 on the cells taken for analysis at 6 or 8 h because active virus alone inhibited host cell RNA and protein syntheses by that time (8, 33).

At various intervals after infection, the overlaid medium was replaced with methionine-free MEM containing 25 μCi of [^{35}S]methionine (to label proteins) or 50 μCi of [^{3}H]uridine (to label RNA) per ml. After a 30-min labeling period, cytoplasmic extracts were prepared for electrophoresis.

Polyacrylamide slab gel electrophoresis of RNA. RNA was extracted from the cytoplasm as previously described (21, 33). The final LiCl-precipitated pellet, free of double-stranded RNA or DNA, was dissolved at a concentration of 200 to 1000 μg/ml in 2 mM phosphate-buffered formamide containing 30% glycerol (formamide sample buffer). The phosphate salts were added directly to the deionized formamide in amounts that gave a pH of 7.0 in aqueous solvents (5). Slab gels consisting of 3.5% acrylamide in 20 mM phosphate-buffered formamide were cast in a Hoefer slab gel apparatus (30 cm by 15 cm by 1.5 mm). Samples containing approximately 6 μg of RNA in 10 μl of sample buffer with 0.01% bromophenol blue were carefully layered under a well filler of 20 mM phosphate-buffered formamide. Electrophoresis was carried out for 20 h at 20°C at 180 V with a buffer of 0.04 M sodium phosphate, pH 7.0.

The gel was cut at the position of the tracking dye and fixed for 1 h in a solution of 1% lanthanum acetate in 1% acetic acid (1) and then impregnated with 20% 2,5-diphenyloxazole (scintillation grade) in dimethyl sulfoxide according to Bonner and Laskey (3). The gel was dried under vacuum with a Hoefer gel-drying apparatus, covered with Saran wrap, and exposed to presensitized Kodak RP X-ray film at −70°C for various periods of time (18).

Polyacrylamide gel electrophoresis of proteins. Protein samples were prepared from the cytoplasmic extracts (8), and approximately 20 to 30 μg of protein (80,000 cpm of [^{35}S]methionine) was layered in each well of a 10-cm 5 to 15% acrylamide–0.1% sodium dodecyl sulfate (SDS) gradient slab gel with a 3% stacking gel. The gel was electrophoresed in 0.05 M Tris-glycine buffer, pH 8.3, for 6 h at 60 V and fixed in a solution of 10% trichloroacetic acid–1% glycerol for 1 h. After they were dried, the gels were exposed to X-ray film at room temperature for 2 to 5 days.

DNA:RNA hybridization. About 100 μg of RNA (specific activity, 10,000 to 20,000 cpm/μg), extracted from the cytoplasm of infected cells, was hybridized to two 24-mm nitrocellulose filters bearing 100 μg of denatured FV 3 or FHM DNA each (27) for 24 h at 37°C in a solution containing 30% formamide, 1.2 M NaCl, 0.12 M sodium citrate, and 0.1% SDS. The filters were rinsed several times in 100 ml of the hybridization buffer. The hybridized RNA was eluted with 1 ml of 99% formamide–0.1% SDS at 50°C for 10 min and diluted 1:1 with 0.2 M sodium acetate buffer, pH 5.4. The RNA was precipitated overnight at −20°C with 3 volumes of absolute ethanol and 100 μg of carrier yeast RNA. The RNA pellet was collected by centrifugation (30 min, 20,000 × *g*) and was dissolved in formamide sample buffer for electrophoresis.

Molecular weight determinations of RNAs and proteins. Molecular weights of each of the viral RNA and protein bands were calculated by comparing the distance migrated with the R_f of the following standards: 28S FHM rRNA, molecular weight, 2

$\times 10^6$; 18S FHM rRNA, 7.08×10^5; 23S *Escherichia coli* rRNA, 1.07×10^6; 16S *E. coli* rRNA, 5.5×10^5; 5S FHM rRNA, 3.5×10^4; 4S FHM tRNA, 2.5×10^4; and reovirus genomic RNA denatured in 99% formamide for 15 min at 37°C – $L_{1,2,3}$, average molecular weight, 1.2×10^6; M_1, 7.6×10^5; $M_{2,3}$, average molecular weight, 7.08×10^5; S_1, 4.7×10^4; S_2, 3.8×10^4; S_3, 3.3×10^4; and S_4, 3.09×10^4. FHM cellular RNAs were assumed to be comparable to similar species from mammalian cells (26). Labeled reovirus RNA was prepared by growing reovirus in L cells for 3 days in the presence of 5 μCi of [^{3}H]uridine per ml. Virions were purified (30), and single-stranded reovirus RNAs were prepared by denaturation in 99% formamide (15 min, 37°C). The molecular weights were taken to be one-half of the values determined for double-stranded RNA segments (30). The distance migrated by the standards was proportional to the logarithm of the molecular weight (5) and was used to derive a fit for the curve $y = ae^{bx}$ by the method of least squares. The resultant curve, $y = 6.06\,e^{-0.00167x}$, where y = log molecular weight and x = migration distance, had a determination coefficient (r^2) of 0.962. The molecular weights of viral proteins were determined in a similar fashion with the following standard proteins; β-galactosidase, 130×10^3; lactoperoxidase, 90×10^3; bovine serum albumin, 67×10^3; ovalbumin, 44×10^3; carbonic anhydrase, 29×10^3; and cytochrome *c*, 12.4×10^3. The resulting best-fit curve, of the type $y = ax + b$, was $y = -0.16x + 5.54$, where y = log molecular weight and x = distance migrated. The coefficient of determination (r^2) equaled 0.99.

Computer analysis of data. The computer analysis was similar to that described by Honess and Roizman (13) for herpesvirus proteins. The developed films were scanned with an Ortec 4310 densitometer interfaced with a PDP 8/1 minicomputer (Digital Electronics Corp.). With the densitometer operating in the percent transmission mode, the analog voltage output generated by the darkened films was changed to digital information by an analog-digital converter (sampling rate of 250 points per s) and stored on magnetic tape. The computer program converted the digital data into absorbance values, corrected base-line levels, displayed the scans on an oscilloscope (Tektronic, Inc. type 611 storage unit), and integrated the selected peaks (see Fig. 3, bottom right panel).

The operator determined the points of inflection on either side of the peaks by inspection of the oscilloscope screen and instructed the computer to mark them with an arrow. The program was designed to integrate the entire area under the peak from the corrected base line. The area of minor bands was determined by scanning longer exposures (96 h) and relating the areas to a reference peak within the limits of resolution of both 36- and 96-h exposures. The same rationale was followed with 24-h exposures to ascertain the areas of the heaviest bands, which exceeded the linear capability of the film during the 36-h exposure.

RESULTS

Separation and characterization of infected cell RNAs. Previous results with sucrose gradients indicated that the synthesis of a 17S viral RNA increased quantitatively with time after infection (33), but this method was not precise enough to measure the rate of synthesis of individual RNA molecules. Using the technique of polyacrylamide gel electrophoresis in formamide coupled with fluorography of the gels, we determined the number of virus-specific RNA species and the relative amounts of each that were labeled during a 30-min pulse with [^{3}H]uridine at various intervals throughout the infectious cycle. Monolayers of FHM cells were treated with ΔFV 3 to suppress host RNA synthesis and were then superinfected with active virus as described above. RNA was extracted from the cytoplasm and analyzed by polyacrylamide gel electrophoresis under denaturing conditions (98% formamide). Figure 1 shows that radioactive bands of RNA were not detected with as much as 10 μg of cytoplasmic RNA extracted from cells receiving only ΔFV 3 for 4 h (Fig. 1a); inhibition of host cell RNA synthesis was maximum by this time.

We assigned molecular weights to the viral RNAs based on their migration distance relative to standards (see above). The infected cell RNA (ICR) number represents the molecular weight $\times 10^3$. Only the molecules of present interest are labeled in Fig. 1, but a composite diagram of all the ICRs ultimately identified is included for reference in Fig. 2. The molecular weights of the infected cell RNAs ranged from 52,000 to 950,000. Many, but not all, of the viral RNAs were synthesized at 1 h after infection (Fig. 1b). By 2 h (Fig. 1c), 47 bands of RNA could be resolved, although not all of them are apparent on the 36-h exposure in Fig. 1. With a

FIG. 1. *Fluorogram of polyacrylamide gel containing RNAs from FV 3-infected cells. RNA, labeled for 30 min with [^{3}H]uridine at various times after infection, was extracted from the cytoplasm of infected cells as described in the text. From 3 to 10 μg of RNA was placed in each well for a total of 40,000 cpm. An exception was the extract from cells receiving only ΔFV 3, in which 10 μg of RNA (4,000 cpm) was used. ΔFV 3 treatment was not necessary for 6- or 8-h samples, because by that time active virus alone had sufficiently reduced host synthesis. Marker RNA was prepared from uninfected FHM cells that had been grown for 3 days in the presence of 0.1 μCi of [^{14}C]uridine per ml; to retain the 4S tRNA species, we did not precipitate this RNA with LiCl. The film was exposed for 36 h at −70°C. (a) 4-h ΔFV 3; (b) 3-h ΔFV 3, 1-h active FV 3; (c) 3-h ΔFV 3, 2-h active FV 3; (d) 3-h ΔFV 3, 4-h active FV 3; (e) 6-h active FV 3; (f) 8-h active FV 3; (g) 6-h FV 3 RNA hybridized to and eluted from FV 3 DNA; (h) uninfected FHM RNA.*

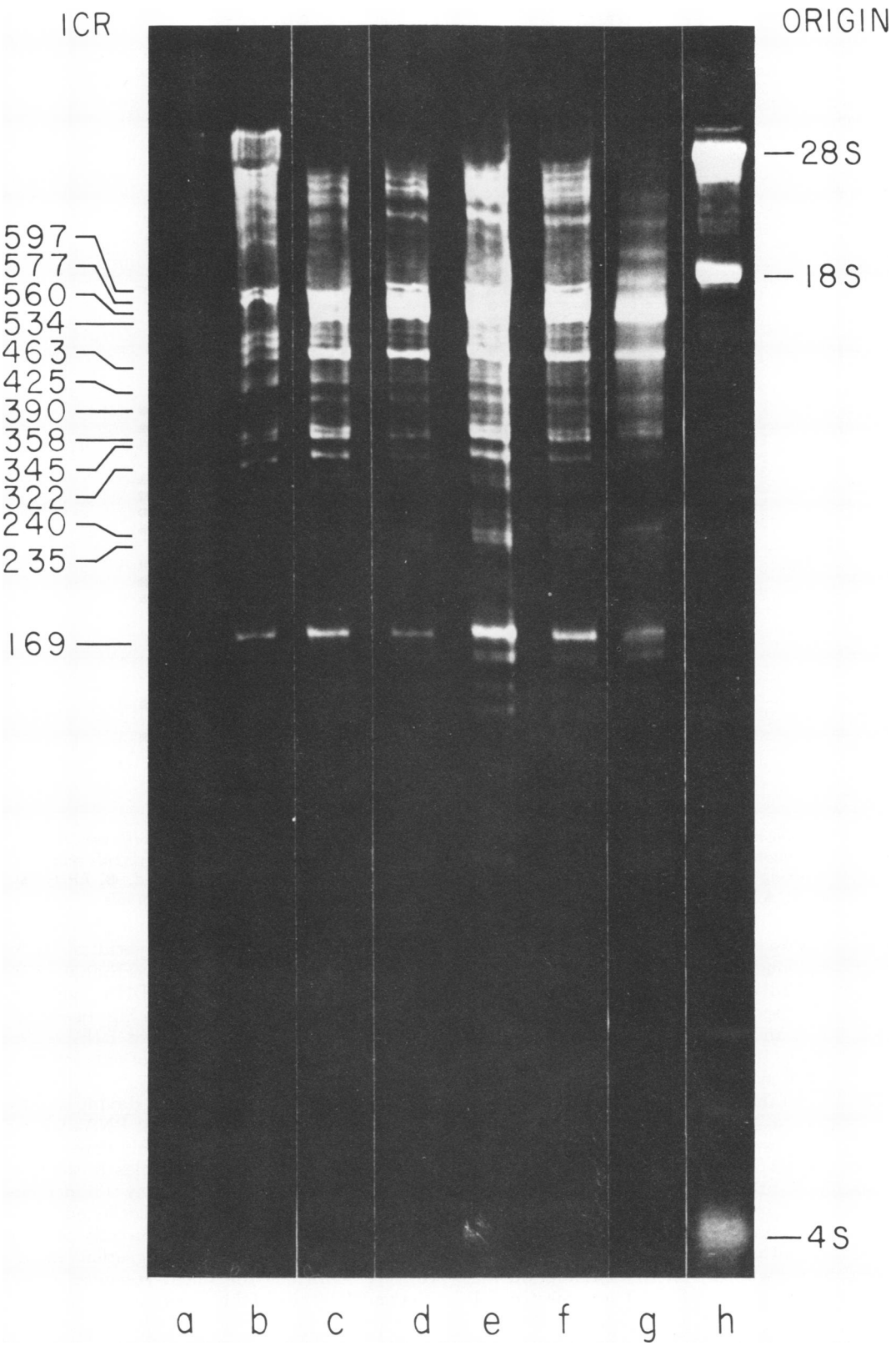
ICR
ORIGIN
28S
18S
4S
597
577
560
534
463
425
390
358
345
322
240
235
169
a
b
c
d
e
f
g
h

FIG. 1.

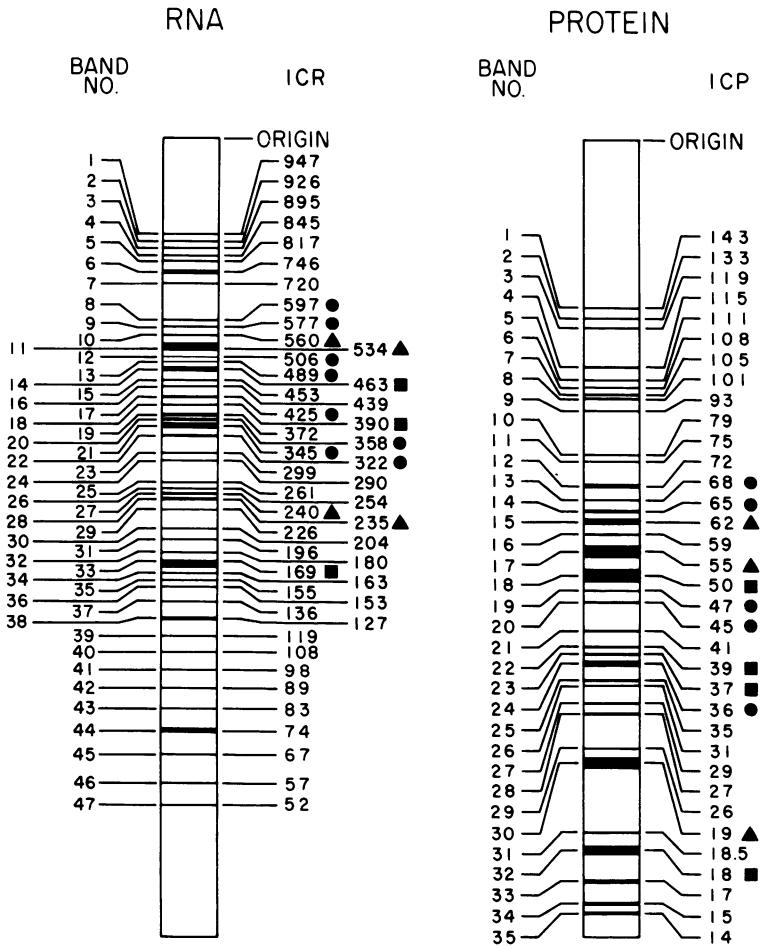

FIG. 2. *Schematic representation of ICRs and ICPs. This drawing is a composite of all bands seen on both short- and long-term exposures of polyacrylamide gels and at every interval examined. The symbols represent the time during the virus growth cycle at which various ICPs are maximally synthesized. ●, Early; ■, intermediate; ▲, late. The ICRs postulated to code for the ICPs were assigned identical symbols.*

96-h exposure (data not shown), the radioactive disintegrations in the major bands exceeded the linear capability of the film. No new viral RNA bands were seen at 4, 6, or 8 h after infection (Fig. 1d, e, and f).

From Fig. 1 it appears that the viral RNAs were not all synthesized at the same rate and that some of them—ICR 560, 534, 390, 240, and 235 (bands 10, 11, 18, 27, 28, and ▲ on the Fig. 2 schematic)—were not synthesized in detectable amounts at 1 h after infection. As the RNA molecules synthesized in infected cells had no counterparts in cells receiving only ΔFV 3, we presumed that these molecules were induced by infection and were coded for by the viral genome. Direct support for this assumption was provided when we subjected an infected cell RNA to electrophoresis after hybridization to and elution from FV 3 DNA. Less than 0.5% of the RNA hybridized to FHM DNA, whereas 35% hybridized to viral DNA. As Fig. 1g shows, most of the prominently labeled RNA molecules that were seen in extracts of cells infected for 6 h hybridized to viral DNA.

Molar ratios of viral RNA. Having shown that the synthesis of many viral RNAs varied with time, we next quantitatively determined the relative number of molecules present in each band. Bonner and Laskey (3) demonstrated that the density of the blackened areas of an exposed X-ray film was directly proportional to the radioactive disintegrations in the gel. We confirmed the linear response of the film and determined the upper and lower limits

of resolution with graded amounts of known standards (see above). The voltage output of our Ortec densitometer during a scan of the film was then converted to digital information and displayed on an oscilloscope (Fig. 3). The total scan was divided into four sections; each section was expanded, and the areas under the peaks were integrated by the computer (13). ICR-577 (early) and ICR 169 (intermediate) are pointed out in the 1-h scan. ICR 534, a late message, is just to the right of ICR 577, but was not detected until 2 h. The pattern established by 4 h did not change thereafter.

The molar ratios of the RNA bands at each time interval are given in Table 1. All values were normalized to that of ICR 322 (band 22), which was defined as 1 unit at 1 h after infection. This band was chosen because it was easily seen on all exposures and did not show extreme variations in rate of synthesis with time. Some bands (e.g., ICR 235/240) that could be distinguished visually were not resolved by the densitometer, and their areas were combined. The minor bands smaller than ICR 127 were not included in Table 1 because the gels were too long to be scanned conveniently in this region. The relative molar rates of synthesis, or molar ratios, were calculated as described in the explanation of Table 1 (13).

Important features of the data in Table 1 are as follows: (i) at 1 h after infection there was, at most, a fivefold difference in the molar rates of synthesis of most of the observable RNA species. ICR 169 (band 33) and, possibly, ICR 577 (band 9) might be considered in relative excess. In addition, several RNA species that became prominent later in infection – notably ICR 560, 534, 390 (bands 10, 11, 18), and all ICR smaller than 169 – were not detected at 1 h, even in long-term exposures.

(ii) By 2 h after infection, the rate of synthesis of the three largest RNA molecules (ICR 895 to ICR 947) declined slightly as compared with the smaller species. Bands undetected in 1-h extracts were now observed, with ICR 560 (band 10) and particularly ICR 534 (band 11) showing marked increases. Although ICR 169 (band 33) was still being synthesized at a rapid rate, the predominant species was now ICR 463 (band 14).

(iii) After 4 h of infection, a characteristic pattern of RNA synthesis emerged that did not change thereafter (Fig. 3). More molecules of ICR 534 were synthesized than any other RNA species. Whereas at 1 h there was a fivefold difference in the molar rates of synthesis between the rarest molecules (ICR 240/235) and the most abundant (ICR 169), at 4 h ICR 534 had become the most abundant RNA species and was synthesized at 50 times the rate of ICR 947, the scarcest 4-h species. At 4 h after infection there was also a greater difference noted in the molar ratios of all other RNA molecules than was observed at 1 h.

(iv) The overall rate of RNA synthesis began to decline 6 h after infection, but several individual species, ICRs 453/439, 390, 358, 345, 322, 240/235, 155/153, and notably ICR 169, reached their peak rate of synthesis at this time (Table 1).

The wide variation seen in the molar ratios of viral RNAs synthesized over the course of the reproductive cycle indicates that complex quantitative transcriptional controls operate in FV 3-infected cells, whereas the appearance of new RNA species 2 h after infection suggests that qualitative controls are important also.

Viral RNAs synthesized in the presence of fluorophenylalanine. If a viral protein induced the changes in the RNA profile that occurred between 1 and 4 h, then interference with the synthesis of functional proteins should lock viral RNA synthesis into a 1-h pattern. The amino acid analog fluorophenylalanine (FPA) is incorporated into proteins that become nonfunctional if a phenylalanine residue is required for activity (28). Since FPA does not actually inhibit protein synthesis, it can be used to study the necessity of early virus-induced proteins for subsequent protein, as well as for RNA, synthesis. Figure 4 shows that 1 h after infection only 10 ICR bands were prominent in the extracts from both untreated (Fig. 4b) and FPA-treated (Fig. 4c) cells, although a few other large-molecular-weight RNAs were faintly visible. By 6 h after infection the typical "late" RNA pattern was seen in extracts of untreated cells (Fig. 4d), but the cells infected in the presence of FPA (Fig. 4e) synthesized the same 10 RNAs at the same rate as at 1 h (Fig. 4b). These results imply that a viral protein(s), normally synthesized within the first hour or two of infection, was required for the characteristic changes in the patterns of RNA synthesis that were observed from 1 to 4 h.

Separation and characterization of viral polypeptides. In earlier reports from this laboratory, Goorha and Granoff (8) identified 20 virus-specific polypeptides with cylindrical polyacrylamide gels. They observed both a class of "early" proteins that reached a high rate of synthesis at 2 h (and thereafter declined) and a class of "late" proteins that did not attain a maximal rate of synthesis until 6 to 8 h.

Because of the improved resolution of proteins obtained on gradient slab gels, we reanalyzed the infected cell polypeptides (ICP) and determined the rates of synthesis of individual

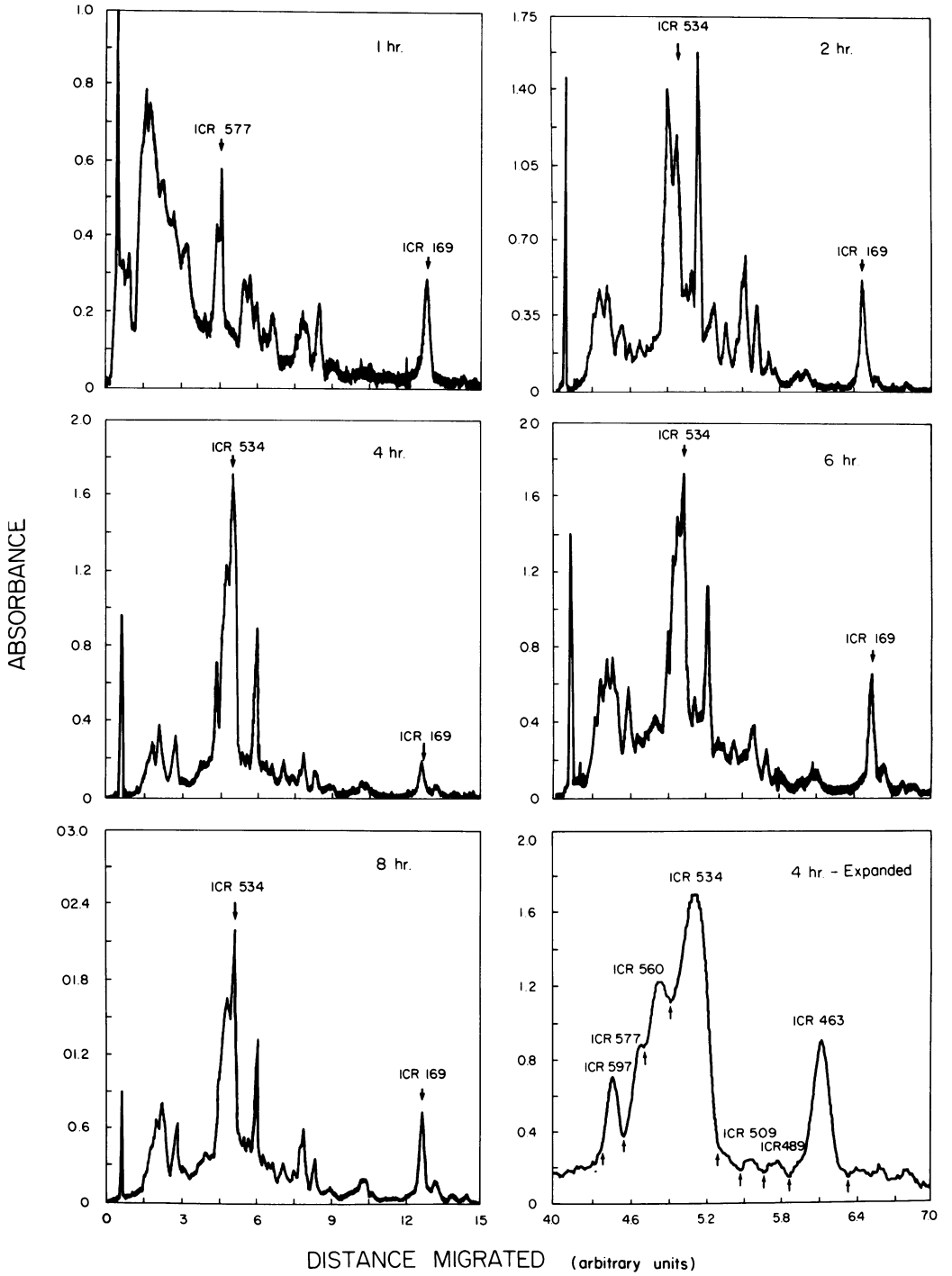

FIG. 3. *Absorbance tracings of fluorograms of viral RNA. The fluorograms of Fig. 1 were scanned by an Ortec densitometer interfaced to an analog-digital converter. The image projected by the computer on the oscilloscope was photographed with a Polaroid camera and reproduced artistically. Labeled peaks are ICR 577, early; ICR 169, intermediate; and ICR 534, late. The sharp line at the beginning of the scan represents a line drawn 2 cm from the origin. The bottom right panel shows an expanded portion of the 4-h sample from 4 to 7 migration units; arrows demarcate the limits of integration, which the computer extended to the base line.*

TABLE 1. *Molar ratios of viral RNAs synthesized at various times after infection*[a]

Band no.	ICR mol wt ($\times 10^3$)	Molar ratio (h)				
		1	2	4	6	8
1	947	1.10	0.22	0.44	0.44	0.63
2	926	1.22	0.49	0.62	0.79	1.14
3	895	2.10	0.82	0.56	1.80	1.39
4	845	1.88	0.65	2.07	1.79	1.77
5	817		0.66	0.62	1.32	1.26
6	746	1.73	0.96	1.63	1.92	1.93
7	720	1.50	0.48	0.63	0.97	1.16
8	597	1.28	1.34	3.50	2.49	2.15
9	577	2.44	3.00	4.64	5.14	4.80
10	560	ND	2.02	9.84	6.60	5.26
11	534	ND	2.17	23.65	14.54	9.76
12	506	1.42	0.96	1.46	1.84	1.69
13	489	1.55	1.30	1.54	2.26	1.54
14	463	1.30	4.65	7.05	6.81	5.43
15	453	0.63	0.97	0.79	1.29	0.65
16	439					
17	425	1.36	0.92	0.91	1.05	0.75
18	390	ND	0.92	1.46	2.35	1.33
19	372	ND	0.57	0.74	1.37	1.13
20	358	0.95	0.77	0.73	2.00	1.44
21	345	0.75	0.97	1.33	3.63	1.74
22	322	1.00	0.96	1.57	2.57	1.46
23	299	ND	0.62	1.18	1.28	1.09
24	290	ND	0.65	2.96	0.81	0.73
25	261	ND	0.68	0.98	1.67	1.05
26	254					
27	240	0.57	0.72	2.03	3.22	2.09
28	235					
29	226	ND	0.33	0.37	0.57	0.81
30	204	ND	ND	ND	ND	ND
31	196	ND	ND	ND	ND	ND
32	180	ND	0.43	0.69	1.10	0.49
33	169	3.16	4.19	5.01	10.10	8.25
34	163	ND	0.64	0.70	1.16	0.85
35	155	ND	0.87	2.51	3.68	2.55
36	153					
37	136	ND	ND	0.85	1.25	1.08
38	127	ND	0.98	1.16	1.23	1.30

[a] Molecular weights were calculated from their relative migration distance compared with the standards as discussed in the text. Molar ratios were calculated according to the formula $MR = K \cdot 10^5 \frac{AiF}{Mi \sum_{Ai-An}}$, where K is the overall rate of RNA synthesis at the time of the determination expressed as a function of the highest observed rate, A and M are the absorbance of band i and its molecular weight, respectively, F is a factor normalizing all values so the ICR 322 equals 1 unit at 1 h after infection, and 10^5 is a constant. ND, None detected via densitometer.

polypeptides from densitometric scans of the autoradiogram. Figure 2 is a composite diagramatic representation of the 35 ICPs detected; molecular weights ranged from 14,000 to 143,000. Figure 5 is an autoradiograph of a gel after electrophoresis of [^{35}S]methionine-labeled proteins extracted from cells at different times after infection. Not all of the 35 viral polypeptides were detected on this exposure; the numbered ICPs are among those whose rates of synthesis varied over the course of infection and were presumed to be regulated. Because the band numbers differed from those previously published, we assigned each protein an ICP number according to its calculated molecular weight $\times 10^3$. Several previously undetected features of the regulation of FV 3 protein synthesis became apparent after we examined these autoradiograms. (i) Better resolution of large-molecular-weight proteins was obtained on slabs than on cylindrical gels; 16 species larger than ICP 55 (Fig. 2, band 17) were sepa-

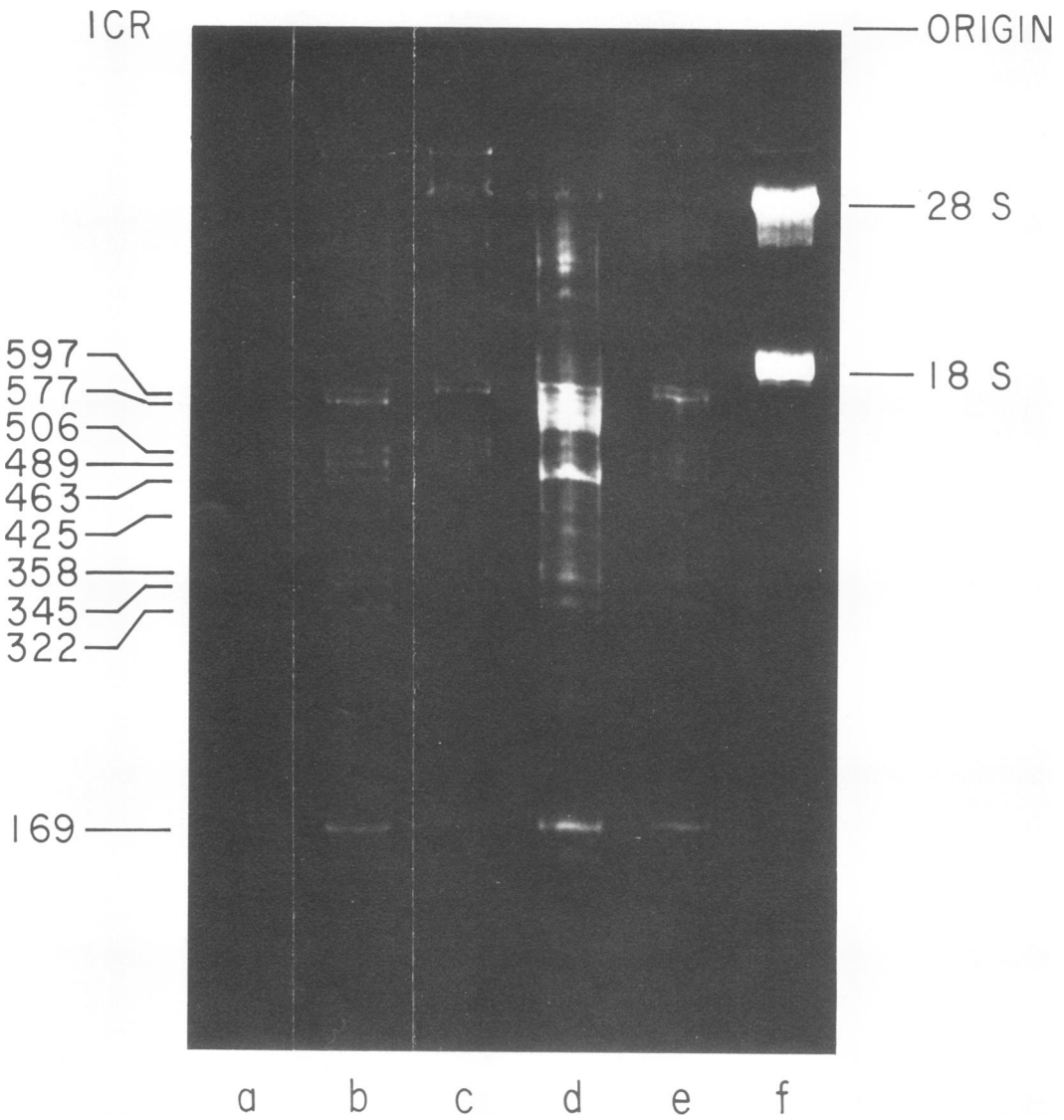

FIG. 4. *Fluorogram of gel containing RNAs from cells infected in the presence of FPA. Monolayers of FHM cells were treated with ΔFV 3 for 4 h before infection with 50 PFU of active FV 3 per cell. The medium did not contain phenylalanine. FPA was present throughout infection in the indicated cultures. Cultures were labeled with 50 μCi of [³H]uridine per ml at 1 to 1.5 or 6 to 6.5 h after infection with active virus. RNAs were extracted and subjected to electrophoresis as described in the text, and the film was exposed for 48 h at −70°C. (a) 5-h ΔFV 3; (b) 4-h ΔFV 3, 1-h active FV 3; (c) same as (b) but with 100 μg of FPA per ml added at 0 h of infection with active virus; (d) 6-h FV 3; (e) same as (d) but with 100 μg of FPA per ml added at 0 h; (f) uninfected FHM RNA (3-day label).*

rated from purified virus (Fig. 5a), whereas before we only saw 4 proteins in this region. (ii) In addition to the "early" and "late" protein classes identified on cylindrical gels, we observed a third or "intermediate" class of proteins whose maximal rate of synthesis was at 4 h (Fig. 5c). (iii) If the cells were treated for 5 h with ΔFV 3 (Fig. 5f), there was a small amount of residual host protein synthesis, primarily of molecules with molecular weights of 50,000 and 17,500. The 17,500-molecular-weight polypeptide just below ICP 18 was considered a host protein because its rate of synthesis at 2 h after superinfection (Fig. 5b) was the same as in the

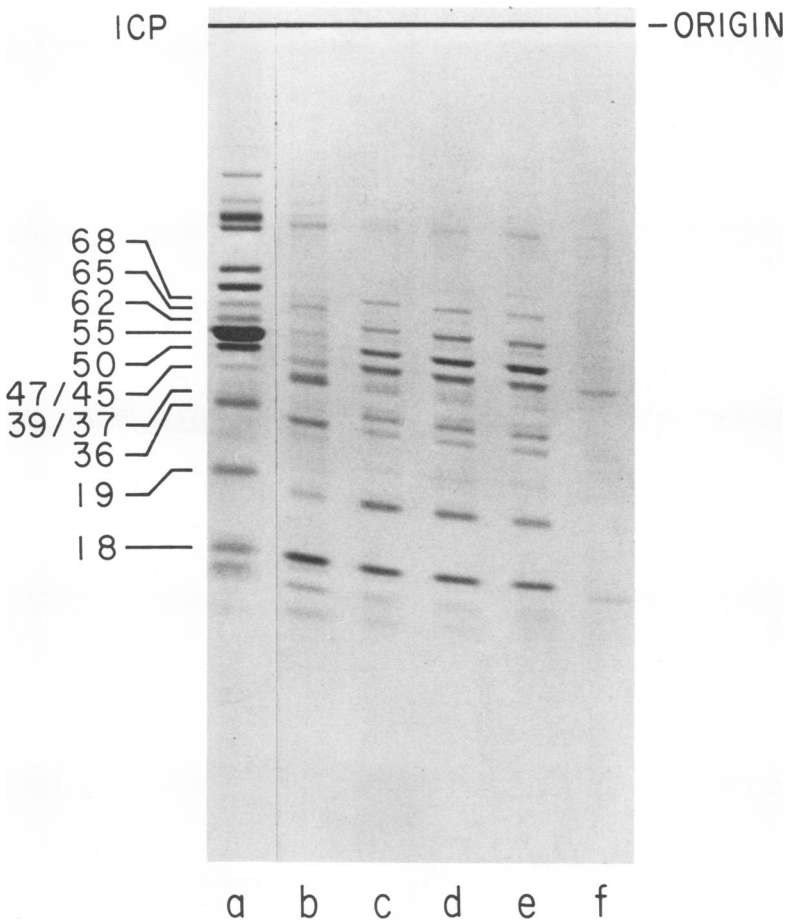

FIG. 5. *Autoradiogram of polyacrylamide gel containing virus-specific polypeptides from FV 3-infected cells. Proteins were labeled for 30 min with 25 μCi of [^{35}S]methionine per ml, and the cytoplasmic extracts were prepared and subjected to electrophoresis as described in the text. From 6 to 30 μg of protein (80,000 cpm) were placed in each well. The film was exposed for 72 h at 23°C. (a) Purified FV 3 structural proteins, 30 μg; (b) 3-h ΔFV 3, 2-h active FV 3; (c) 3-h ΔFV 3, 4-h active FV 3; (d) 6-h active FV 3; (e) 8-h active FV 3; (f) 5-h ΔFV 3. Heat-inactivated virus was not used for 6- or 8-h samples, because active virus alone inhibited host cell protein synthesis at that time.*

heat-inactivated control (Fig. 5f). This band was not given an ICP number. ICP 50 (Fig. 2, band 18) had a small host component, but the polypeptide was considered to be predominantly viral in origin because its rate of synthesis increased with time after infection (Fig. 5c, d, and e).

To obtain quantitative data, we scanned the autoradiographs with an Ortec densitometer (Fig. 6) and instructed the computer to integrate the areas under the peaks; the molar ratios are presented in Table 2. Almost one-half of the detectable viral proteins were synthesized at maximal rates early in infection (1 or 2 h). These include ICPs 115, 118, 105/101, 93, 68, 65, 59, 47/45, 36, 35/31, 17, 15, and 14. The late proteins—ICPs 62, 55, and 19 (bands 4, 17, and 30)—were barely detectable at 1 or 2 h but rose to high rates of synthesis late in infection (6 h). The newly identified third class of "intermediate" proteins (ICPs 79, 75, 50, 39/37, 29/27, 26, 18, and 17) reached their highest rate of synthesis at 4 h. ICP 18 (band 32) was always produced in greater quantities than any other protein, but the rate of synthesis dropped 50% between 4 and 8 h after infection. ICP 18, the most abundant product of translation, and ICP 55, a late protein that is the most prominent viral structural protein, are identified on the densitometric tracings in Fig. 6. The proteins that we clas-

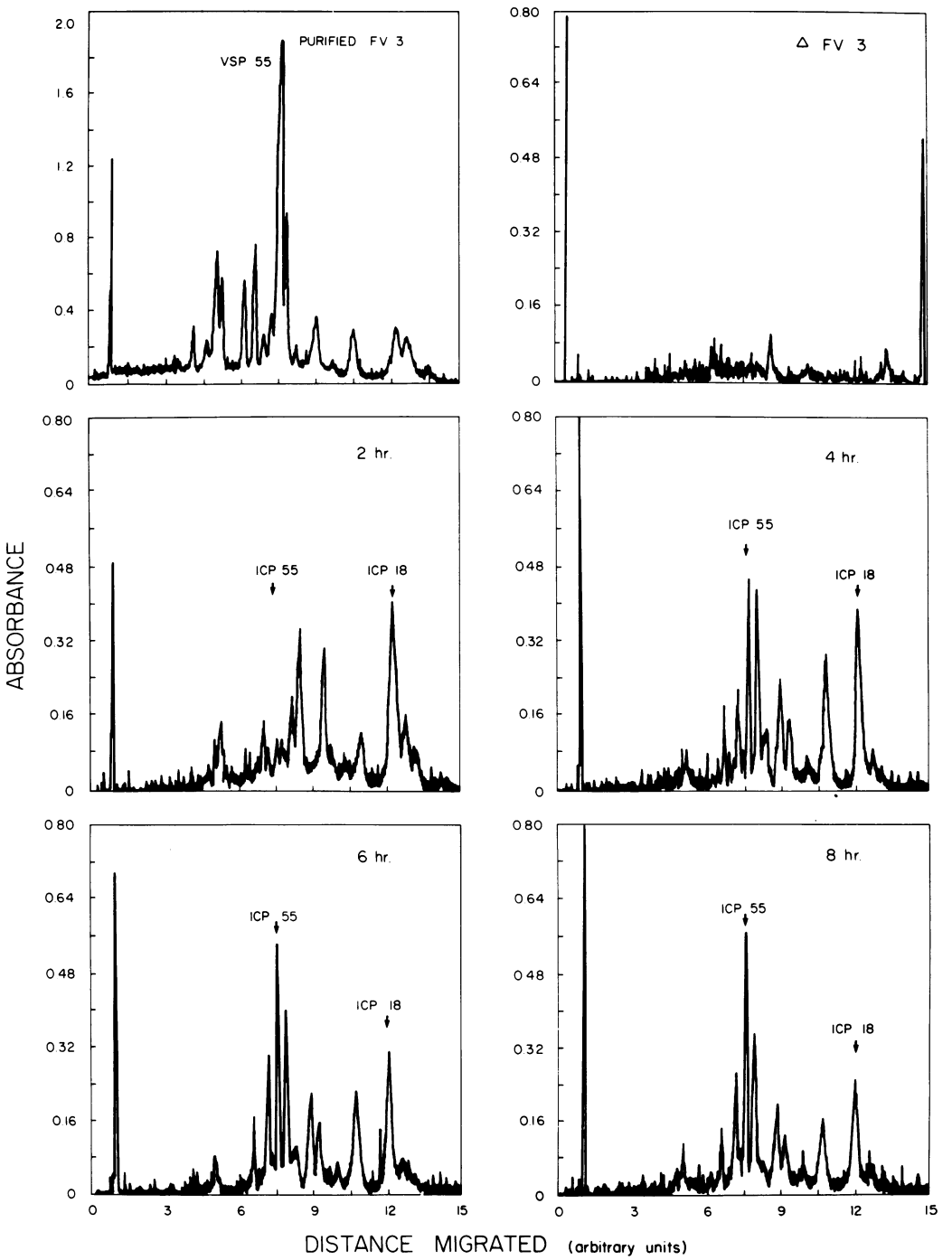

FIG. 6. *Absorbance tracings of autoradiograms of viral proteins. Details as in legend to Fig. 3. The labeled peaks are ICP 18, intermediate; and ICP 55, late. VSP, Viral structural protein.*

sified as early and intermediate displayed decreased molar rates of synthesis after 2 and 4 h of infection, respectively (Table 2). Table 1 shows no similar reduction in the rate of synthesis of most of the early RNAs. The continued high rate of synthesis of early and intermediate RNAs extends the earlier work of Goorha and Granoff (9), who suggested that the inhibition

TABLE 2. *Molar ratios of viral polypeptides synthesized at various times after infection*[a]

Band no.	ICP mol wt ($\times 10^3$)	Molar ratio (h)				
		1	2	4	6	8
1	143	ND	ND	ND	ND	ND
2	133	0.015	0.032	ND	ND	ND
3	119	0.011	0.025	ND	ND	ND
4	115	0.030	0.09	ND	ND	ND
5	111	0.115	0.20	ND	ND	ND
6	108	0.088	0.24	0.24	0.11	0.19
7	105	0.104	0.88	0.61	0.54	0.59
8	101					
9	93	0.12	0.25	ND	ND	ND
10	79	0.12	0.24	0.30	0.21	0.13
11	75	0.19	0.48	1.10	0.96	0.71
12	72	ND	ND	ND	ND	ND
13	68	0.47	1.18	0.47	0.34	ND
14	65	0.37	0.65	0.50	0.40	0.24
15	62	ND	0.40	2.36	2.89	2.4
16	59	0.29	1.0	0.68	0.79	0.75
17	55	0.39	1.08	4.8	5.71	5.7
18	50	1.01	2.46	7.3	5.69	4.47
19	47	2.10	7.2	3.78	1.73	0.76
20	45					
21	41	ND	ND	ND	ND	ND
22	39	0.61	1.82	6.75	5.53	4.38
23	37					
24	36	1.64	6.12	4.38	3.57	2.83
25	35	0.76	2.72	1.20	1.32	ND
26	31					
27	29	0.75	2.58	3.18	1.98	1.4
28	27					
29	26	ND	1.20	2.86	1.79	ND
30	19	0.63	5.88	12.99	16.96	8.4
31	18.5	ND	ND	ND	ND	ND
32	18	4.32	20.65	26.48	16.3	12.0
33	17	0.65	5.2	5.41	2.76	ND
34	15	0.49	10.59	5.93	4.93	2.23
35	14	1.27	6.16	2.52	ND	ND

[a] Molecular weights were calculated from relative migration distances compared to standard proteins as described in the text. The molar ratios were determined according to the formula given in the footnote to Table I; the term F normalized all data to ICP 59 at 2 h postinfection. ND, Nondetectable by densitometer.

of at least one early protein took place at the post-transcriptional level.

Viral polypeptides synthesized in the presence of FPA. If the RNA species synthesized after infection in the presence of FPA were the true early viral mRNA's, and FPA did not inhibit their translation, then the viral polypeptides synthesized in the presence of FPA should represent the translation products of these RNAs. Figure 7 shows that viral polypeptides synthesized after 6 h of infection in the presence of FPA (Fig. 7e) were the same ones that were synthesized early in infection in the absence of drug (Fig. 7b). Some of these polypeptides (ICPs 68, 65, 50, 47/45, 39/37, 36, 18) were the right size to be translation products of the specific early RNAs synthesized in the presence of FPA (Fig. 4e; ICRs 597, 577, 463, 425, 358, 345, 169). The polypeptides that were not observed after 6 h of infection in the presence of FPA but were readily detected after infection in the absence of drug (Fig. 7d; ICPs 62, 55, 19) were the right size to have been coded for by RNAs that only appeared if functional protein synthesis was permitted (Fig. 4d; ICRs 560, 534, 240/235). This result strengthens the proposed coding correlation between those RNAs and proteins.

DISCUSSION

Correlation of specific viral RNAs and proteins. We have shown that virus-specific RNAs isolated from cells infected with a large DNA virus, FV 3, can be resolved into at least 47 component bands by polyacrylamide gel electrophoresis in formamide. The molecular weights of the viral RNAs ranged from 52,000 to 947,000, whereas the molecular weights of the viral polypeptides ranged from 14,000 to

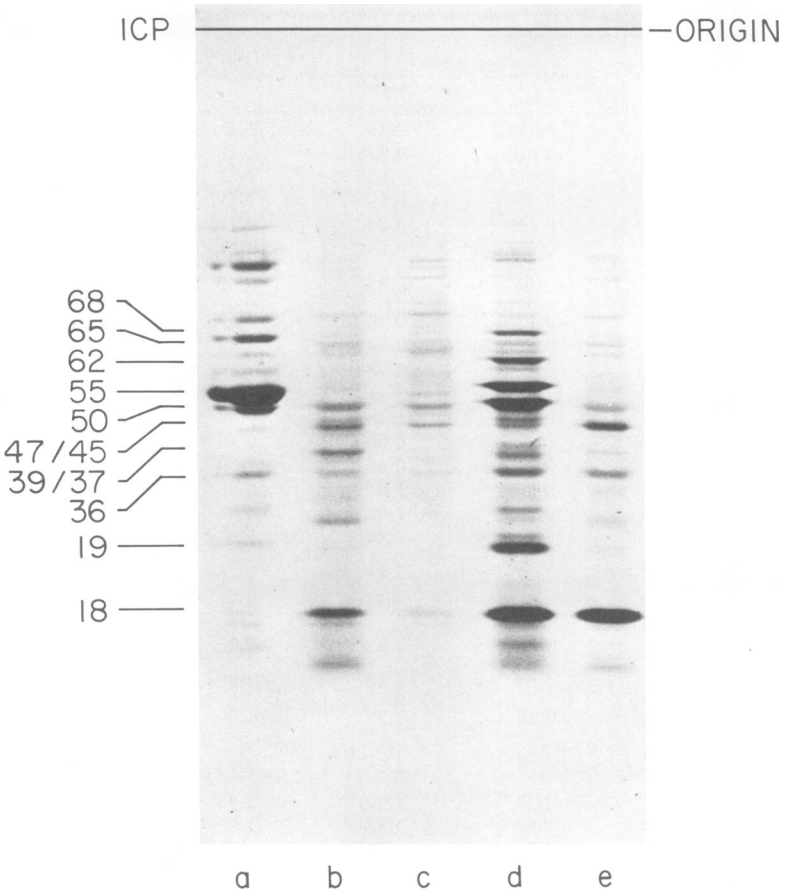

FIG. 7. *Autoradiogram of gel containing polypeptides from cells infected in the presence of FPA. Monolayers of FHM cells were infected as described in the legend to Fig. 5. Polypeptides were labeled for 30 min with 25 μCi of [^{35}S]methionine per ml, and the cytoplasmic extracts were prepared and subjected to electrophoresis as described in the text. (a) Purified FV 3 structural proteins; (b) 3-h ΔFV 3, 1-h active FV 3; (c) same as (b) but with 100 μg of FPA per ml added at 0 h of infection; (d) 6-h active FV 3; (e) 6-h active FV 3 with 100 μg of FPA per ml added at 0 h of infection.*

143,000. Only 40% of the single-stranded genome equivalent was accounted for from the total molecular weight of the RNAs determined directly from the RNA electrophoresis or calculated from the molecular weights of the proteins. Therefore, some of the bands of both RNA and protein probably contained two or more molecular species. Slight errors in molar ratio determinations were also introduced by the integration process, which did not distinguish overlap into neighboring peaks.

One of the goals of this investigation was to identify selected RNA bands as the messengers for specific viral polypeptides by size and by coordinate temporal behavior in rates of synthesis, and thereby to assist in explaining the control mechanisms used by this virus. The size of the mRNA necessary to code for each of the polypeptides was calculated assuming the amino acid residue to have a molecular weight of 100 and the nucleotide that of 300. This assumption seems reasonable because FV 3 mRNA has no poly(A) tracts (34), and we have not found any evidence of either glycosylation or post-translational cleavage of viral polypeptides (unpublished data). Vesicular stomatitis virus mRNA (32) and reovirus mRNA (4) have both been translated in vitro and appear to possess no large untranslated regions. The segments of the influenza virus genome are also the right size to code for the influenza proteins (29).

Table 3 lists 10 RNA:protein pairs for which we presently have reasonably good circumstantial bases for assigning a relationship, such as size, rate of synthesis, and synthesis in the

presence of FPA. Four pairs are early, three are intermediate, and three are late. All of the calculated and observed molecular weights are within a range of ±10%.

In Fig. 8, we have plotted the relative rates of synthesis at various times after infection of the RNAs and proteins selected for Table 3. A further discussion of these data will be found in the sections on transcriptional and post-transcriptional regulation. We recognize the limitations of the data in the estimation of molecular weights and assignment of particular RNAs as messages for particular proteins. Nevertheless, until isolated FV 3 mRNA's are translated in vitro and the products are identified as FV 3 polypeptides, the postulated protein relationships provide a foundation for useful discussion. Although some of the RNA to protein correlations may be incorrect, our interpretation of the data regarding post-transcriptional control is unambiguous.

Regulation at the level of transcription. The data presented in Table 1 suggest that transcription is regulated in both a qualitative and quantitative manner. With the exception of ICR 169 (band 33) and ICR 577 (band 9), most of the RNAs seen at 1 h postinfection (Fig. 4b) or after 6 h in the presence of FPA (Fig. 4e) were produced in approximately equimolar amounts—at most there was only a three- to fourfold difference in the molar rates of synthesis of any of the other species. By 4 h after infection not only were additional species being synthesized, but there was also as much as a 50-fold differential between the relative molar rates of synthesis of the most scarce and the most abundant RNAs. More molecules of ICR 534 (band 11) were made than of any other viral RNA. We consider this RNA to be the messenger for the major viral structural protein, ICP-55 (band 17), because of its size and rate of synthesis.

These results support our earlier hybridization studies (33), which demonstrated the existence of both temporal and abundance controls of viral RNA synthesis. The new techniques, however, allow us to give attention to the behavior of specific molecular species.

We identified three viral RNAs (ICRs 560, 534, and 240/235) that could potentially code for three late proteins, ICPs 62, 55, and 19 (Table 3). These ICRs were not detected at 1 h postinfection and were inhibited by FPA. The small amount of ICR 240/235 synthesis that was observed under these conditions could be explained if one of these bands was the mRNA for a protein other than ICP 19.

In Fig. 8 (bottom panel) we show that the rates of synthesis of both late RNAs and proteins accelerated to about the same degree during infection. This concomitant increase indicates that synthesis of late proteins was regulated at the level of transcription.

Regulation at the level of translation. The results clearly demonstrate the importance of post-transcriptional control in the switch-off of early and intermediate protein synthesis in FV 3-infected cells. The only RNAs whose molar rate of synthesis declined with time were the large-molecular-weight species, ICR 947 through ICR 817 (Table 1). There was also a decrease in molar ratios of the largest infected

TABLE 3. *Correlation of FV 3-specific mRNA's and proteins*

ICP mol wt[a] (×10³)	Classification	RNA-calculated[b] mol wt (×10³)	ICR[b] mol wt (×10³)	RNA synthesized in presence of FPA
68	Early	612	597	+
65	Early	585	577	+
47/45	Early	405, 423	425	+
36	Early	324	345	+
50	Intermediate	450	463	+
39/37	Intermediate	333, 351	358	+
18	Intermediate	162	169	+
62	Late	558	560	0
55	Late	495	534	0
19	Late	270	240, 235	0

[a] Molecular weights of proteins were determined by relative mobility compared with standards in SDS-polyacrylamide gels.

[b] Molecular weights of RNAs required to code for such proteins were calculated from an average amino acid molecular weight of 100 and that of 300 for nucleotides, with three nucleotides per amino acid. Observed molecular weight of RNAs (ICR) were determined by electrophoretic mobility in formamide-polyacrylamide gels as described in the text.

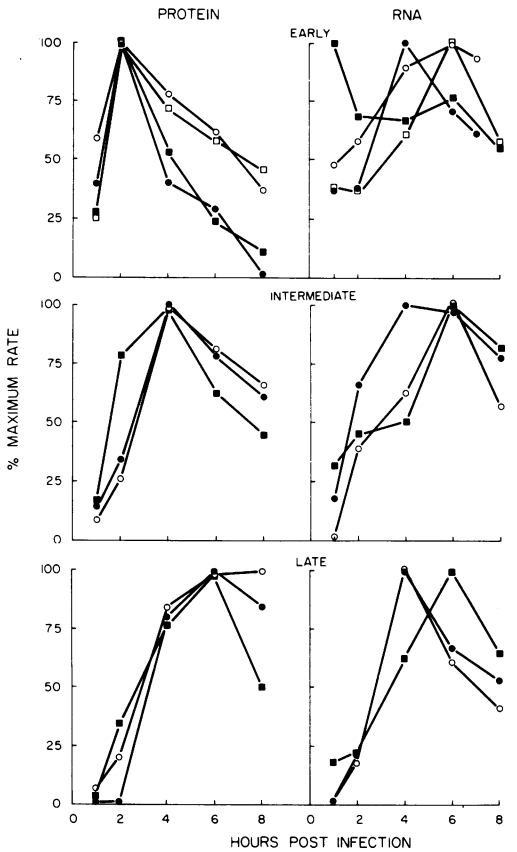

FIG. 8. *Molar rate of synthesis of early, intermediate, and late FV 3 RNAs and proteins. The values are expressed as percentage of the maximum molar rate of synthesis. Identical symbols are used for the polypeptide and its presumptive mRNA. Early proteins: ICP 68, ●; ICP 65, ○; ICP 47/45, ■; ICP 36, □. Early RNAs: ICR 597, ●; ICR 577, ○; ICR 425, ■; ICR 332, □. Intermediate proteins: ICP 50, ●; ICP 39/37, ○; ICP 18, ■. Intermediate RNAs: ICR 463, ●; ICR 358, ○; ICR 169, ■. Late proteins: ICP 62, ●; ICP 55, ○; ICP 19, ■. Late RNAs: ICR 560, ●; ICR 534, ○; ICR 240/235, ■.*

cell proteins (ICP 133 through ICP 111, Table 2), whose rates of synthesis might, therefore, be negatively controlled at the transcriptional level. All RNAs smaller than ICR 746 continued to be synthesized at 4 and 6 h after infection at rates comparable to or greater than those established at 2 h.

The seven RNAs assigned the coding potential for the early and intermediate proteins (Table 3) were of the correct size and met the additional criterion of being synthesized in the presence of FPA. The rate of RNA synthesis for the four early proteins did not decrease between 2 and 6 h and, in all but one instance, showed a definite increase (Fig. 8). Therefore, if these RNAs are the actual messages for these proteins, a negative control must operate at the post-transcriptional level.

The RNAs assigned to the three intermediate proteins also continued to be synthesized at an increased rate at 6 h, whereas from 4 to 6 h the synthesis of the corresponding proteins went down, again implicating post-transcriptional control (Fig. 8).

Goorha and Granoff (9) have presented evidence for the post-transcriptional regulation of ICP 18 (then termed VSP 13). The present report supports their findings by demonstrating that the rate of synthesis of ICR 169, the presumptive mRNA for ICP 18, remains high throughout infection (Fig. 8).

General significance of this study. Most of the experimental evidence favors transcriptional control as the primary mode of regulation by DNA bacteriophage and by both RNA and DNA animal viruses (2, 7, 17, 19, 23, 24, 31, 32). The classical hypothesis on control of transcription by DNA viruses was established by investigators who used hybridization data to divide RNA qualitatively into early and late categories, depending on time of initiation of viral DNA synthesis. An element of qualitative transcriptional control was also apparent in FV 3-infected cells, but in this system a virus-induced protein, rather than DNA synthesis per se (8), was required to turn on late transcription.

After analyzing the kinetics of DNA:RNA hybridization in liquid, Frenkel and Roizman (6) postulated quantitative control of transcription in herpesvirus-infected cells; Wold et al. (35) did the same with adenovirus. Such experiments inform us only of the number of abundance classes of RNA that differ by 10-fold. We have provided direct evidence for a more varied quantitative control of FV 3 RNA synthesis. Separation of FV 3 RNA on polyacrylamide gels clearly demonstrates that the molecular species were not all synthesized at the same rate at any specified time and that the same size classes were synthesized at different rates at different times.

A paramount finding of this study was the key role of post-transcriptional regulation in the viral growth cycle; over one-half of the detectable infected cell polypeptides appeared to be regulated at this level. The evidence for translational control in eucaryotic systems has accumulated slowly over the years since McAuslan (20) first demonstrated that vaccinia virus-induced thymidine kinase synthesis was not switched off in the presence of actinomycin

D. Honess and Roizman (14, 15) suggested a "cascade" regulation of herpesvirus-specific proteins. As they found early herpesvirus RNAs present late in infection, Frenkel and Roizman (6) postulated post-transcriptional regulation for the switch-off of early herpesvirus proteins. Oppermann and Koch (25) have also strengthened the hypothesis for translational control in eucaryotic virus infection by demonstrating that messages for the prereplicative polypeptides of vaccinia virus persisted late in infection. However, a simultaneous comparison of the rates of synthesis of individual viral RNA species with those of viral polypeptides synthesized throughout the infectious cycle was only achieved with FV 3. Our data demonstrate that early RNAs are not only present late in infection but are still actively being synthesized, despite an apparent inability to be translated. Therefore, there is no negative control of most of the early FV 3 RNAs. The proof that a particular protein is specified by a particular RNA will be provided when isolated viral RNAs are translated in vitro, and we now have the means to accomplish this. We will then assay for the factors that regulate translation, eg., of ICP 18.

ACKNOWLEDGMENTS

We wish to thank Frank Morris of the Department of Electrical Engineering at Memphis State University for his invaluable aid in the computer analysis. Ramona Tirey and Susan Carr provided skilled technical assistance.

This research was supported by a research project grant CA 07055 and a Childhood Cancer Research Center Grant CA 08480 from the National Cancer Institute and by ALSAC.

LITERATURE CITED

1. **Adesnik, M.** 1971. Polyacrylamide gel electrophoresis of viral RNA, p. 126-175. *In* K. Maramorosch and H. Koprowski (ed.), Methods in virology, vol. 18. Academic Press Inc., New York.
2. **Aloni, Y., E. Winocour, and L. Sachs.** 1968. Characterization of the simian virus 40-specific RNA in virus-yielding and transformed cells. J. Mol. Biol. 31:415-429.
3. **Bonner, W. M., and R. A. Laskey.** 1974. A film detection method for tritium-labeled proteins and nucleic acids in polyacrylamide gels. Eur. J. Biochem. 46:83-88.
4. **Both, G. W., S. Lavi, and A. J. Shatkin.** 1975. Synthesis of all the gene products of the reovirus genome *in vivo* and *in vitro*. Cell 4:173-180.
5. **Duesberg, P. H., and P. K. Vogt.** 1973. Gel electrophoresis of avian leukosis and sarcoma viral RNA in formamide: comparison with other viral and cellular RNA species. J. Virol. 12:594-599.
6. **Frenkel, N., and B. Roizman.** 1972. Ribonucleic acid synthesis in cells infected with herpes simplex virus: controls of transcription and of RNA abundance. Proc. Natl. Acad. Sci. U.S.A. 69:2654-2658.
7. **Gage, L., and E. P. Geiduschek.** 1967. Repression of early messenger transcription in the development of a bacteriophage. J. Mol. Biol. 30:435-440.
8. **Goorha, R., and A. Granoff.** 1974. Macromolecular synthesis in cells infected by frog virus 3. I. Virus-specific protein synthesis and its regulation. Virology 60:237-250.
9. **Goorha, R., and A. Granoff.** 1974. Macromolecular synthesis in cells infected by frog virus 3. II. Evidence for post-transcriptional control of a viral structural protein. Virology 60:251-259.
10. **Goorha, R., R. F. Naegele, D. Purifoy, and A. Granoff.** 1975. Macromolecular synthesis in cells infected with frog virus 3. III. Virus-specific protein synthesis by temperature-sensitive mutants. Virology 66:428-439.
11. **Goorha, R., D. Willis, and A. Granoff.** 1977. Macromolecular synthesis in cells infected by frog virus 3. VI. FV 3 replication is dependent on the cell nucleus. J. Virol. 21:802-805.
12. **Granoff, A., P. E. Came, and D. C. Breeze.** 1966. Viruses and renal carcinoma of *Rana pipiens*. I. The isolation and properties of virus from normal and tumor tissue. Virology 29:133-148.
13. **Honess, R. W., and B. Roizman.** 1973. Proteins specified by herpes simplex virus. XI. Identification and relative molar rates of synthesis of structural and nonstructural herpesvirus polypeptides in the infected cell. J. Virol. 12:1347-1365.
14. **Honess, R. W., and B. Roizman.** 1974. Regulation of herpesvirus macromolecular synthesis. I. Cascade regulation of the synthesis of three groups of viral proteins. J. Virol. 14:8-19.
15. **Honess, R. W., and B. Roizman.** 1975. Regulation of herpesvirus macromolecular synthesis: sequential transition of polypeptide synthesis requires functional viral polypeptides. Proc. Natl. Acad. Sci. U.S.A. 72:1276-1280.
16. **Kelly, D. C., and R. J. Avery.** 1974. Frog virus 3 deoxyribonucleic acid. J. Gen. Virol. 24:1-10.
17. **Kourilsky, P., M. Bourguignon, M. Bouquet, and F. Gros.** 1970. Early transcription controls after induction of prophage. Cold Spring Harbor Symp. Quant. Biol. 25:305-314.
18. **Laskey, R. A., and A. D. Mills.** 1975. Quantitative film detection of ^{3}H and ^{14}C in polyacrylamide gels by fluorography. Eur. J. Biochem. 56:335-341.
19. **Lucas, J. J., and H. S. Ginsberg.** 1971. Synthesis of virus-specific ribonucleic acid in KB cells infected with type 2 adenovirus. J. Virol. 8:203-213.
20. **McAuslan, B. R.** 1963. The induction and repression of thymidine kinase in the pox virus-infected HeLa cell. Virology 21:383-389.
21. **Milcarek, C., R. Price, and S. Penman.** 1974. The metabolism of a poly(A) minus RNA fraction in HeLa cells. Cell 3:1-10.
22. **Naegele, R. F., and A. Granoff.** 1971. Viruses and renal carcinoma of Rana pipiens. XI. Isolation of frog virus 3 temperature sensitive mutants; complementation and genetic recombination. Virology 44:286-295.
23. **Nonoyama, M., S. Millward, and A. F. Graham.** 1974. Control of transcription of the reovirus genome. Nucleic Acids Res. 1:373-385.
24. **Oda, K., and W. K. Joklik.** 1967. Hybridization and sedimentation studies on "early" and "late" vaccinia messenger RNA. J. Mol. Biol. 27:395-419.
25. **Oppermann, H., and G. Koch.** 1976. On the regulation of protein synthesis in vaccinia virus infected cells. J. Gen. Virol. 32:262-273.
26. **Peacock, A. C., and C. W. Dingman.** 1968. Molecular weight estimation and separation of ribonucleic acid by electrophoresis in agarose-acrylamide composite gels. Biochemistry 7:668-674.
27. **Raskas, H. G., and M. Green.** 1971. DNA-RNA and DNA-DNA hybridization in virus research, p. 247-269. *In* K. Maramorosch and H. Koprowski (ed.),

Methods in virology, vol. 5. Academic Press Inc., New York.
28. **Richmond, M. H.** 1962. The effect of amino acid analogues in growth and protein synthesis in microorganisms. Bacteriol. Rev. **26**:398–420.
29. **Ritchey, M. B., P. Palese, and J. L. Schulman.** 1976. Mapping of the influenza virus genome. III. Identification of genes coding for nucleoprotein, membrane protein, and nonstructural protein. J. Virol. **20**:307–313.
30. **Shatkin, A. J., J. D. Sipe, and P. Loh.** 1968. Separation of ten reovirus genome segments by polyacrylamide gel electrophoresis. J. Virol. **2**:986–991.
31. **Travers, A. A.** 1969. Bacteriophage sigma factor for RNA polymerase. Nature (London) **223**:1107–1110.
32. **Villarreal, L. P., M. Breindl, and J. J. Holland.** 1976. Determination of molar ratios of vesicular stomatitis virus induced RNA species in BHK_{21} cells. Biochemistry **15**:1663–1667.
33. **Willis, D., and A. Granoff.** 1976. Macromolecular synthesis in cells infected by frog virus 3. IV. Regulation of virus-specific RNA synthesis. Virology **70**:399–410.
34. **Willis, D., and A. Granoff.** 1976. Macromolecular synthesis in cells infected by frog virus 3. V. The absence of polyadenylic acid in the majority of virus-specific RNA species. Virology **73**:543–547.
35. **Wold, W. S., M. Green, K. H. Brackmann, M. A. Cartus, and C. Devine.** 1976. Genome expression and mRNA maturation at late stages of productive adenovirus type 2 infection. J. Virol. **20**:465–477.